

## Differential Si Ring Optical Resonator Biosensors

Tomoya Taniguchi<sup>1</sup>, Yoshiteru Amemiya<sup>1</sup>, Takeshi Ikeda<sup>3,1</sup>, Akio Kuroda<sup>3,1</sup>, and Shin Yokoyama<sup>1,2</sup>

<sup>1</sup>Res. Inst. for Nanodevice and Bio Systems, Hiroshima Univ. <sup>2</sup>Dept of Semiconductor Electronics and Integration

<sup>3</sup>Dept of Molecular Biotechnology AdSM Hiroshima Univ.

1-4-2 Kagamiyama, Higashihiroshima, Hiroshima 739-8527, Japan

Phone: +81-82-424-6265, Fax: +81-82-424-3499, E-mail: yokoyama-shin@hiroshima-u.ac.jp

### 1. Introduction

We are studying biosensors detectable plural kinds reactions rapidly without labeling [1-3]. The schematic structure of the target integrated biosensor is shown in Fig. 1. The Si ring biosensor is compact and suitable for the integration. However, the sensitivity for biosensing is not sufficiently high and the improvement has been done for example by using slot waveguide [2,3]. Figure 2 shows the fabricated ring biosensor with slot waveguide. An example of biosensing using normal Si ring biosensor is shown in Fig. 3 for the prostate specific antigen (PSA) [1]. The sensitivity is  $10^{-7}$  g/ml, while the practically required sensitivity is  $10^{-9}$  g/ml. Further two orders of improvement is required. One order of improvement was achieved by slot waveguide. One more order of improvement is expected by the differential sensing.

### 2. Operation principle of biosensor

Structure of the differential biosensor is shown in Fig. 4. There are two rings (for reference and sensing), and one of the output is connected to  $180^\circ$  phase shifter, and merged again. The measurement principle for the direct sensing is shown in Fig. 5(a). The wavelength of the input laser is fixed at the steepest point of the resonance curve ( $\lambda_{\text{res}} \pm w\sqrt{3}/6$ , where  $\lambda_{\text{res}}$  and  $w$  are resonance wavelength and FWHM, respectively). To increase the sensitivity the quality factor  $Q$  of the ring resonator must be high. However, since the FWHM of the input laser is finite (0.045 nm in this study), the output signal is reduced when  $Q$  becomes high (both signal increase and decrease portions exist within FWHM and cancelled). On the other hand for the differential sensing both of temperature fluctuation and stray light or any common mode noises are cancelled. And also wide FWHM input laser is available.

### 3. Simulated results of differential biosensors

The simulation of the characteristics of the differential and direct biosensors were carried out using the transfer function of the electric field including intensity and phase for the ring resonator [4]. For the differential sensing the wavelength of the input laser was fixed at the resonance wavelength of the reference ring. Figure 6 shows the output power as a function of  $Q$  of the ring. The refractive index change is fixed at  $5 \times 10^{-5}$  which corresponds to the change in resonance wavelength of  $\sim 0.02$  nm. From the Langmuir equation in Fig. 3, this number corresponds to the PSA

concentration of  $8 \times 10^{-9}$  g/ml. Except at small  $Q$  region the differential sensing yields higher output than direct sensing, resulting in higher S/N ratio, e.g. higher sensitivity. Next, the output is simulated as a function of the refractive index change at  $Q=2.26 \times 10^4$  (Fig. 7) (when  $Q$  is too high slight difference between reference and sensing rings saturates the differential output, then the maximum position  $Q=5 \times 10^4$  is avoided). It should be noted that in the differential sensing there is a linear region from  $2$  to  $8 \times 10^{-5}$ , which is a big benefit for parallel operation of sensors with slightly different resonance wavelengths. Figure 8 shows the simulated output at refractive index change of  $5 \times 10^{-5}$  as a function of temperature change. In direct sensing temperature fluctuation must be  $< 50$  m°C for the 1 ng/ml PSA sensing, while for the differential sensing the output change was  $< 10^{-3}$  and gives no effect for sensing.

### 4. Uniformity of resonance wavelength of Si rings

Measured distribution of resonance wavelength of Si ring resonators in 2 inch wafer is shown in Fig.9. The difference between neighboring rings (100  $\mu\text{m}$  far) can be within 0.02 nm, which corresponds within the linear region in Fig. 7. When operation point is set in the middle of the linear region (intentionally the resonance wavelengths of the reference and sensing rings are set different), the biosensing sensitivity is constant even for the scattering of the resonance wavelength exists within this linear region..

### 5. Conclusions

The predominance of the differential biosensor is indicated by the simulation. Especially the temperature stability is excellent and a high tolerance for the scattering of the resonator characteristics is demonstrated.

### Acknowledgement

This study is partially supported by a Grant-in-Aid for Scientific Research (B) (246360136, 2012) from the Ministry of Education, Culture, Sports, Science and Technology of Japan.

### References

- [1] M. Fukuyama *et al.*, Jpn. J. App. Phys. **50** (2011) 04DL07.
- [2] M. Fukuyama *et al.*, Jpn. J. App. Phys. **50** (2011) 04DL11.
- [3] A. Hirowatari *et al.*, Proc. SPIE Photonics Europe 2012, **8431** (2012) 63.
- [4] Y. Kokubun, Oyo Buturi **72** (2003) 1364 [in Japanese].

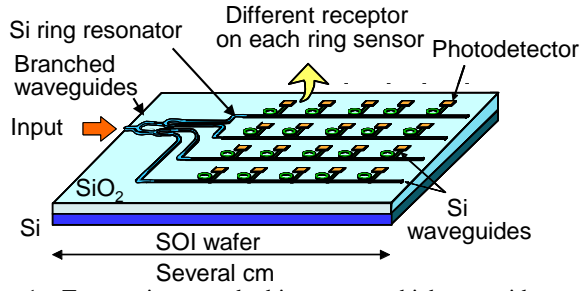


Fig. 1 Target integrated biosensor which provides simultaneous multispecies biosensing. Ring resonator sensors are suitable because of their compactness.

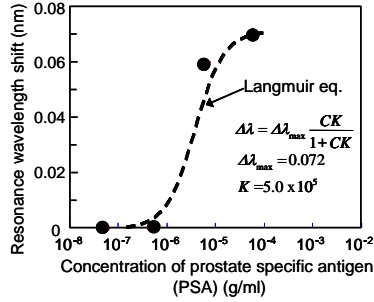


Fig. 3 Resonance wavelength shift of the Si ring biosensor for prostate specific antigen (PSA). The practically required sensing concentration is  $\sim 10^{-9}$  g/ml. Further two orders of magnitude improvement will be achieved by slot ring and differential sensing.

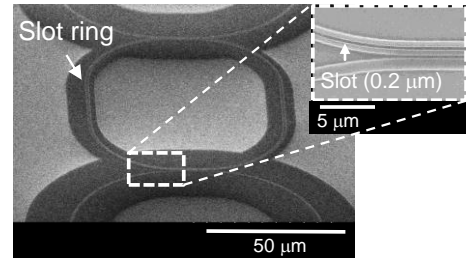


Fig. 2 Scanning electron microscope (SEM) image of the slot ring biosensor fabricated in our lab. The slot (width of 0.2  $\mu\text{m}$ ) is very effective to enhance the sensitivity. However, the further improvement of sensitivity and temperature stability is required before practical use.

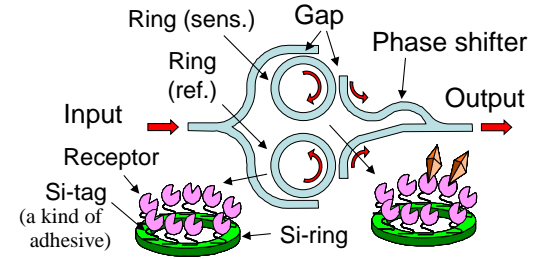


Fig. 4 Proposed differential type ring resonator sensor, which has special features such as high sensitivity due to the common-mode-noise cancellation and high temperature stability by the same temperature dependence of the reference and sensing rings.

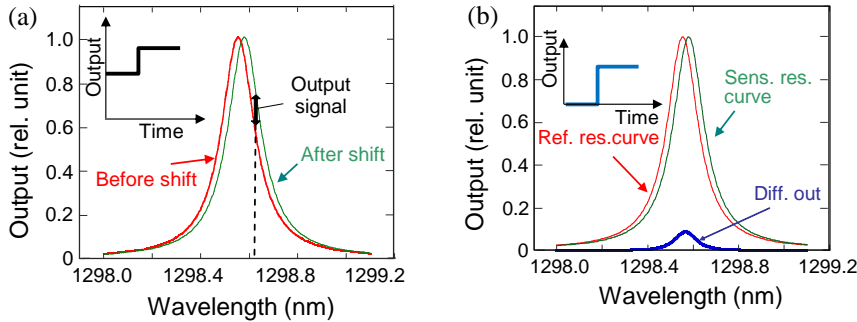


Fig. 5 Principle of biosensing mechanism for (a) previous direct sensing and (b) differential sensing. For direct sensing the temperature fluctuation and stray light cause the serious problem. On the other hand for the differential sensing both of these noise sources are cancelled. The structure is simple: one of the output of two rings are connected to 180° phase shifter, and merged again as shown in Fig. 2.

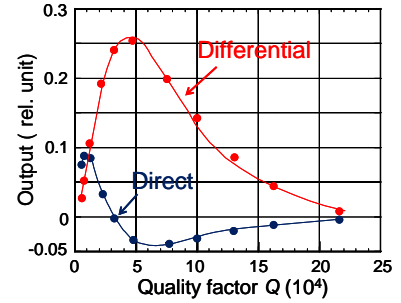


Fig. 6 Simulated output from differential and direct sensors as a function of  $Q$  of the ring. The refractive index change is fixed at  $5 \times 10^{-5}$ . Except at small  $Q$  region the differential sensing yields higher output.

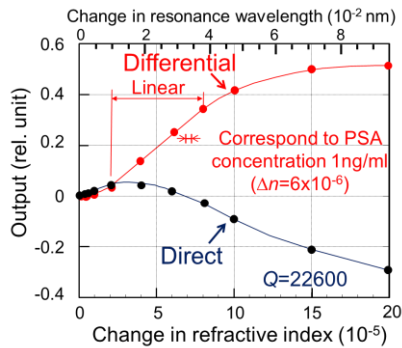


Fig. 7 Simulated output as a function of refractive index change. It should be noted that in the differential sensing there is a linear region from 2 to 8  $\times 10^{-5}$ , the slope is maximum, which is a big benefit for parallel operation of plural sensors with somewhat different resonance wavelengths.

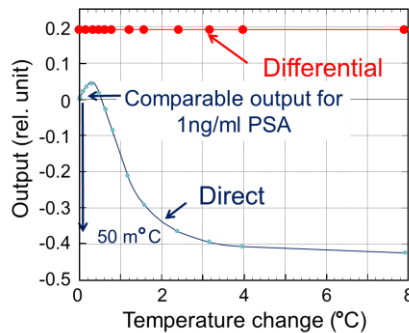


Fig. 8 Simulated output at refractive index change of  $5 \times 10^{-5}$  as a function of temperature change. In direct sensing temperature fluctuation must be less than 50 m°C for the 1 ng/ml PSA sensing, while for the differential sensing the output change is less than  $10^{-3}$ .

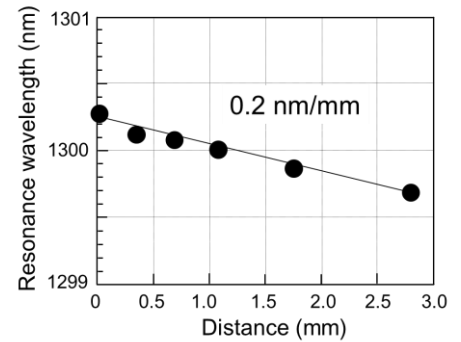


Fig. 9 Measured distribution of resonance wavelength of Si ring resonators in 2 inch wafer. The difference between neighboring rings (100  $\mu\text{m}$  far) can be within 0.02 nm, which corresponds within the linear region in Fig. 7, resulting in equal sensitivity for all differential sensors.